Supplementary Information

Biogenic Growth of Alloys and Core-shell Nanostructures Using Urease as a Nanoreactor at Ambient Conditions

Bhagwati Sharma, Sonam Mandani and Tridib K Sarma*

Discipline of Chemistry, School of Basic Sciences, Indian Institute of Technology Indore

IET Campus, DAVV, Khandwa Road, Indore- 452017, India.

Correspondence: T.K.S (tridib@iiti.ac.in)

EXPERIMENTAL SECTION

Materials. Hydrogen tetrachloroaurate ($HAuCl_4$), Silver nitrate ($AgNO_3$), Potassium tetrachloroplatinate (K_2PtCl_4), Jack Bean urease, Urea, Zinc nitrate hexahydrate, 5,5'-dithiobis(2-nitrobenzoic acid) (DTNB), and 8-Anilino-1-naphthalenesulfonic acid (ANS) were purchased from Sigma- Aldrich. Sodium dihydrogen phosphate monohydrate, di-Sodium hydrogen phosphate, Sodium nitrate and Bromocresol purple were purchased from Merck, India. Potassium carbonate was purchased from Rankem, India. p-nitroaniline and sodium borohydride were purchased from S.D Fine chemicals, India. All the chemicals were used as received without any further purification. Milli Q water was used throughout the experiments.

Synthesis of Au nanoparticles using K_2CO_3. Gold nanoparticles with an average size of 8.9 nm were synthesized using the enzyme urease. In a typical synthesis, 2.5 ml of 2mg/ml enzyme solution, 2.5 mg K_2CO_3 and 50 µL of 0.03 M $HAuCl_4$ were taken in a vial and the reaction mixture was heated at 37° C with mild stirring for 6 hrs. The formation of Au nanoparticles was visualized through their characteristic pink color.

Synthesis of Au nanoparticles using PBS buffer at pH 7.4. 5 mg of urease was dissolved in 2.5 ml of 10 mM PBS buffer of pH 7.4. To it, 50 µL of 0.03 M $HAuCl_4$ was added, and the solution was heated at 37° C with stirring. The characteristic pink color of the Au nanoparticles was observed after 48 hours.

Synthesis of Ag nanoparticles. The synthesis of Ag NPs was similar to that of Au NPs, whereby 25 µL of 0.03 M $AgNO_3$ solution was added to 2.2 ml of 2mg/ml enzyme

solution, containing 0.95 mg K_2CO_3, and the resulting mixture was stirred at 37° C for 6 hrs.

Synthesis of Pt nanoparticles. In a similar procedure, Pt nanoparticles were formed by the reaction of 2.5 ml of 2mg/ml urease solution with 75 µl of 0.02 M K_2PtCl_4 in presence of 2 mg K_2CO_3 and heated at 37° C for 36 hrs.

XPS Measurement. The XPS measurements were performed using an ESCA instrument: VSW of UK make with an Al Kα source, at a resolution of 1eV. The sample was measured in thin film mode by drop casting the nanoparticle solution on a glass slide.

Modification of Thiol groups in Urease using DTNB. The Thiol groups in urease were modified using DTNB in PBS buffer of strength 50 mM and pH 7.8, following a reported procedure[1]. Briefly, 2.5 mg of urease was dissolved in 1.25 ml phosphate buffer. To this solution 1.25 mL of 5 mM DTNB was added. The color of DTNB solution changed from colorless to yellow, indicating the modification of thiol groups after a few minutes.

Conformational changes in urease after nanoparticle synthesis.

Fluorescence Studies

The conformational changes in urease after the synthesis of nanoparticles were studied using an extrinsic fluorophore, ANS. For this purpose, ANS with a final concentration of 20 µM was added to each of native urease solution, Au NP- urease solution and citrate capped Au nanoparticles- urease, and fluorescence spectra were recorded at excitation wavelength of 370 nm, after incubating the solutions in dark for 4 hours.

Circular Dichroism studies

The CD studies were performed at 25 °C on a Jasco-815 spectrometer. Spectra were recorded between 260 and 190 nm with a data pitch of 0.1 nm. The scanning speed was set to 20 nm/ min with band width of 1nm. The path length was 1 mm quartz cell (Starna Scientific Ltd. Hainault, UK). We used an enzyme concentration of 1mg/ml throughout the experiments. Each spectrum is the result of average of three consecutive scans.

Comparison of the activity of the native urease and urease after Au nanoparticles synthesis by pH measurement.

The activity of urease was measured by noting the rise in pH upon addition of urea. For this purpose, 50 mg of urea was added to 10 ml of both native urease (1mg/ml) and urease-Au NP solution, and the increase in pH with time was recorded.

Comparison of the activity of the native urease and urease after Au nanoparticle synthesis using Bromocresol purple.

The activity was also confirmed spectroscopically using the bromocresol purple assay, following a reported procedure.[2] Briefly, two test solutions were taken, one containing native enzyme, 0.015 mM Bromocresol Purple and 0.2 mM EDTA. In the second solution the native enzyme was replaced by Au NP- enzyme composite, and the pH was adjusted to 5.8. Then to the solutions urea was added and absorbance at 588 nm was recorded at various time intervals.

Pertinent equations

The decomposition of urea, resulting in an increase in the pH of the system can be achieved using enzymatic route. The enzyme urease decomposes urea into ammonia and carbon dioxide in aqueous solutions according to the following reactions:

$$CO(NH_2)_2 + H_2O + \text{Urease} \longrightarrow NH_3 + NH_2COOH \quad (1)$$

$$NH_2COOH + H_2O \longrightarrow NH_3 + H_2CO_3 \quad (2)$$

$$H_2CO_3 \longrightarrow CO_2 + H_2O \quad (3)$$

The reducing ability of the enzyme, presumably because of free thiols present in the cysteine residues functions as follows during the metal nanoparticle synthesis:

$$Au^{3+} + R{-}SH \longrightarrow Au^0 + H^+ + R{-}S{-}S{-}R \quad (4)$$

$$R{-}SH + Au \longrightarrow R{-}S{-}Au + 1/_2\, H_2 \quad (5)$$

The free thiols provide the electrons to Au^{3+} (or Ag^+, Pt^{2+}) for reduction as well as protons in the solution, and themselves get converted to disulfides.

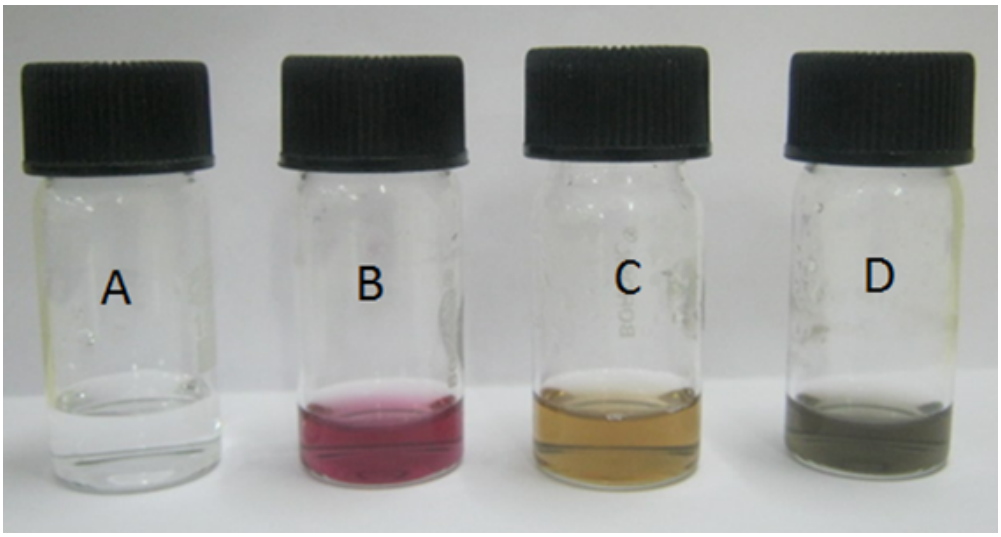

Figure S1. Photograph showing different metal nanoparticles synthesized using urease as both reducing and stabilizing agent. (A) Enzyme solution before reaction and after reaction with (B) $HAuCl_4$, (C) $AgNO_3$ and (D) K_2PtCl_4.

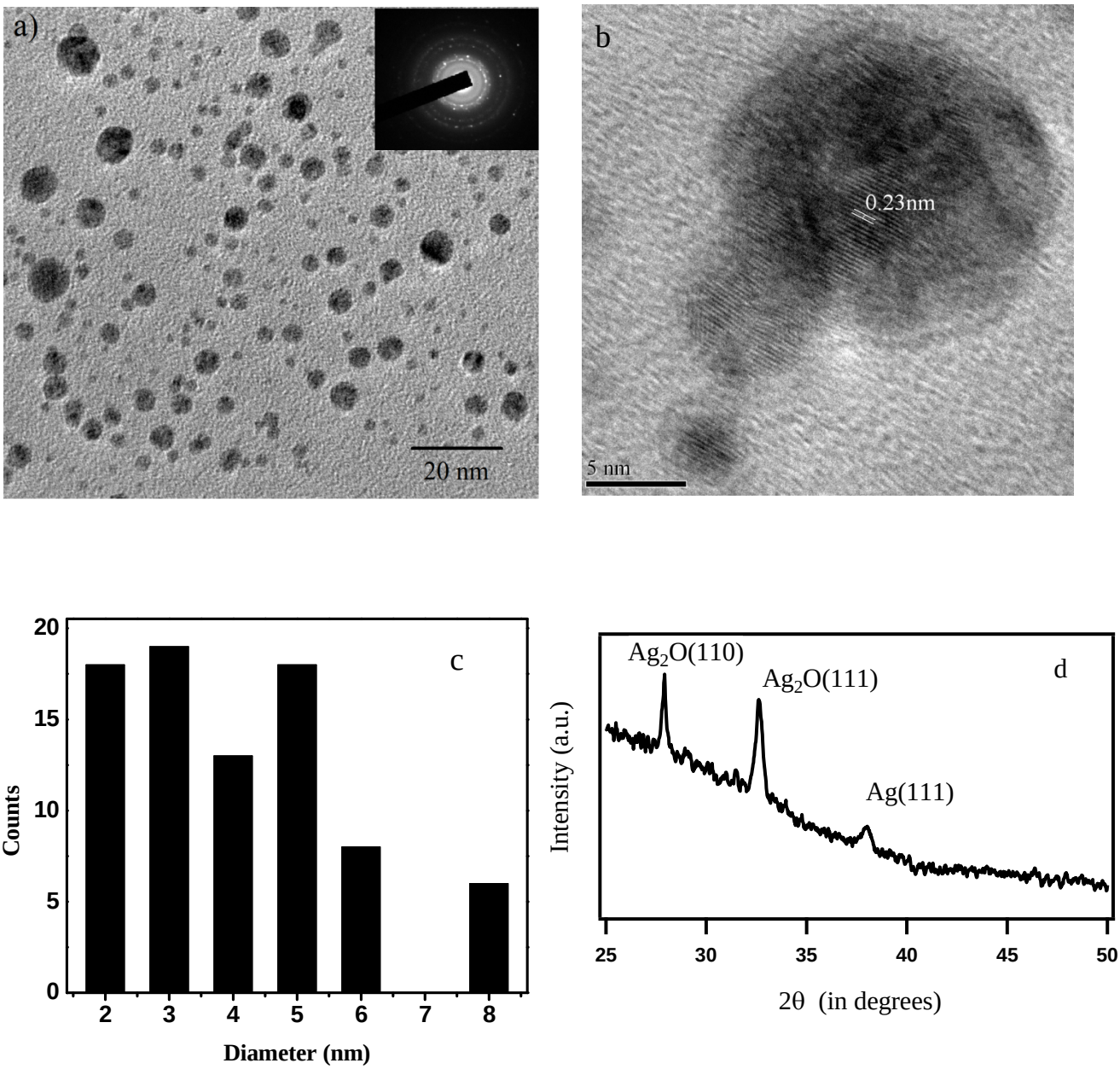

Figure S2. (a) TEM image and SAED pattern (inset) of Ag-Ag_2O composite nanoparticles (b) HR-TEM image (c) particle size distribution and (d) powder XRD spectrum of the synthesized Ag-Ag_2O composite nanoparticles. Principal Braggs' reflection of Ag_2O and Ag are identified.

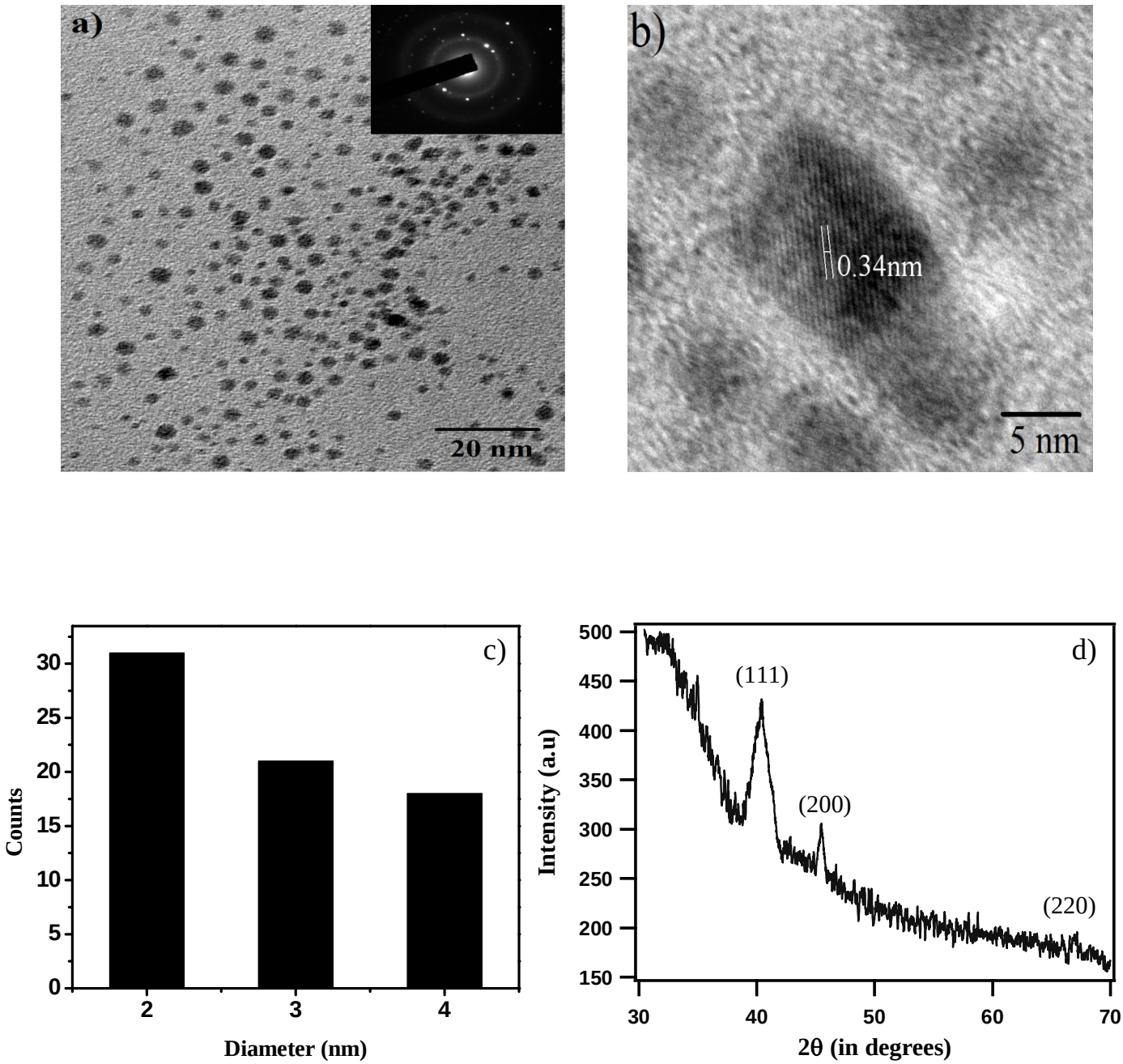

Figure S3. (a) TEM image and SAED pattern (inset) of the Pt nanoparticles, (b) HR-TEM image (c) particle size distribution and (d) powder XRD spectrum of the synthesized Pt nanoparticles.

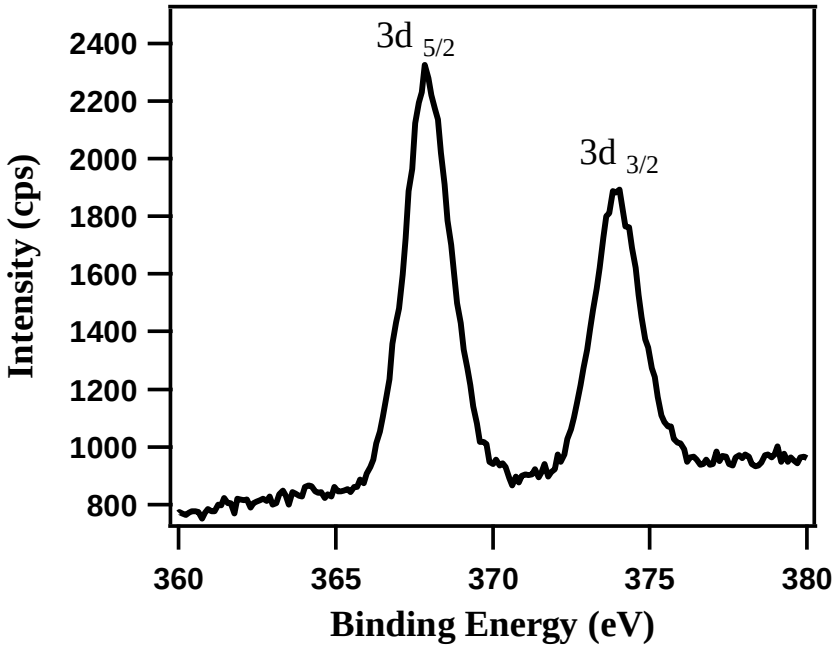

Figure S4. XPS spectrum of 3d electrons of Ag-Ag_2O composite nanostructure.

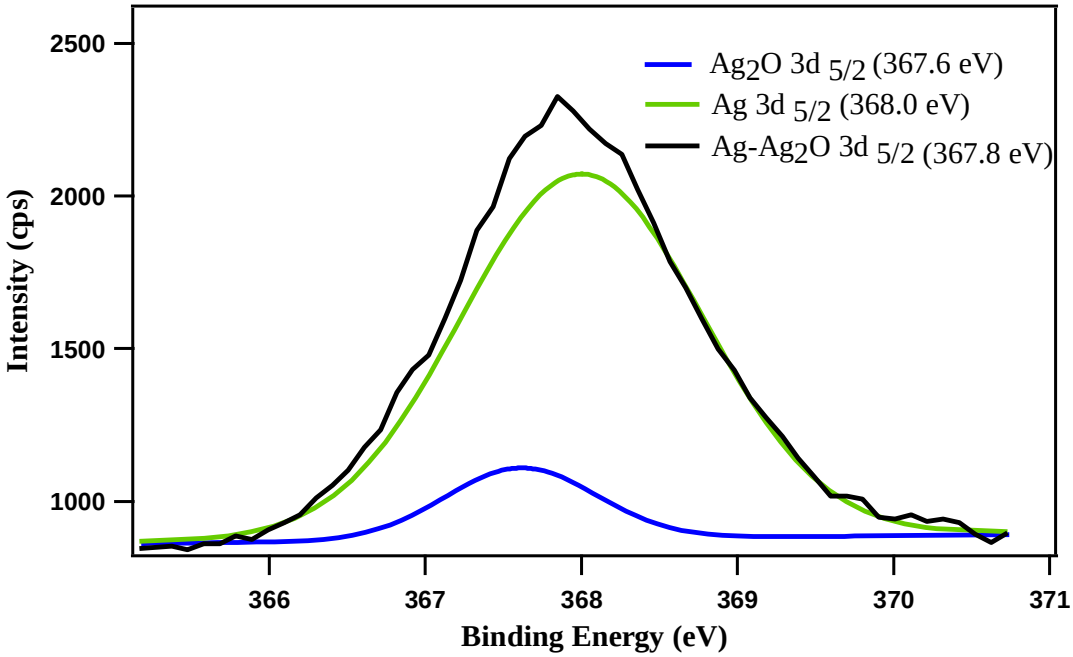

Figure S5. XPS spectrum for Ag 3d $_{5/2}$ photoelectrons, showing the presence of both Ag and Ag_2O.

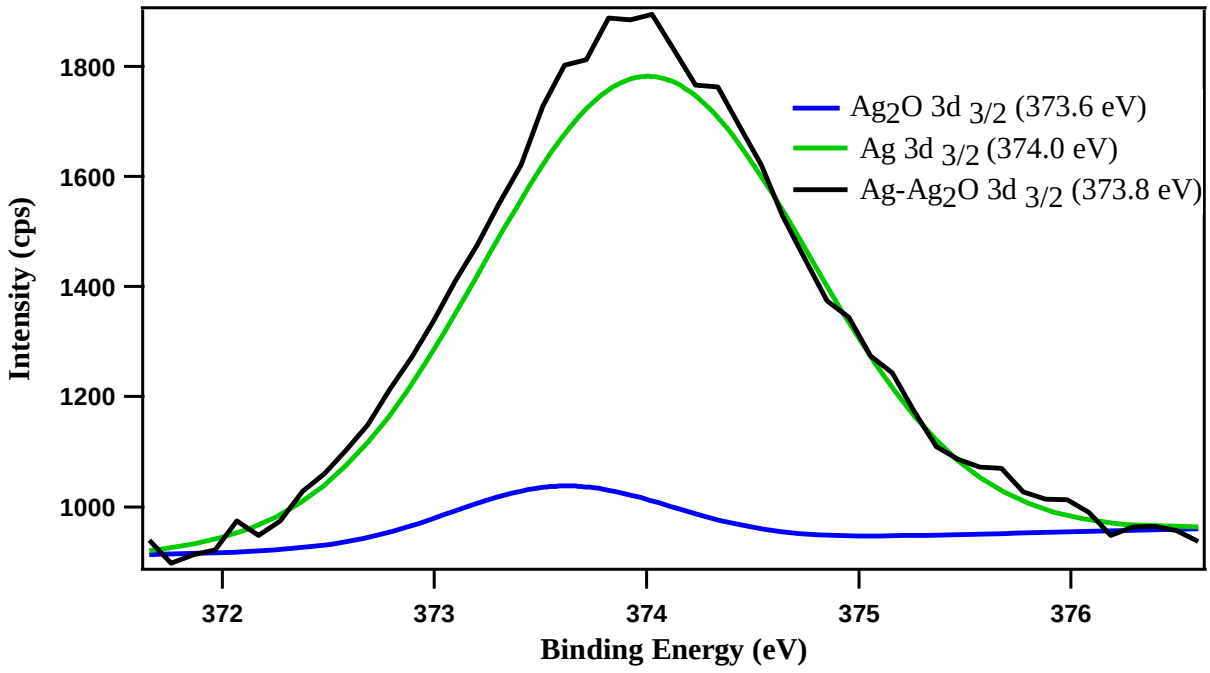

Figure S6. XPS spectrum for Ag 3d $_{3/2}$ photoelectrons, showing the presence of both Ag and Ag_2O.

The core level XPS analysis of the Ag nanoparticles revealed the formation of a minor amount of Ag_2O, along with the Ag nanoparticles, as evidenced from the spectrum of the 3d $_{5/2}$ and 3d $_{3/2}$ electrons. Peaks at binding energies of 367.6 and 368.0 eV corresponding to 3d $_{5/2}$ photoelectrons of Ag_2O and Ag respectively were observed[3,4]. In addition the spectrum also showed peaks at 373.6 and 374.0 eV characteristic of 3d $_{3/2}$ photoelectrons of Ag_2O and Ag respectively[3]. Thus from the XPS analysis it was confirmed that in addition to Ag nanoparticles as major compononent, a minor amount of Ag_2O was also formed. Quantitatively, Ag-Ag_2O nanocomposite consist of 19.42% of Ag_2O and 80.58% of Ag. The Ag_2O layer is on the surface of the Ag nanoparticles, giving rise to a core-shell like morphology. The thickness of the Ag_2O layer on the Ag nanoparticles is in good agreement with previous literature report[5].

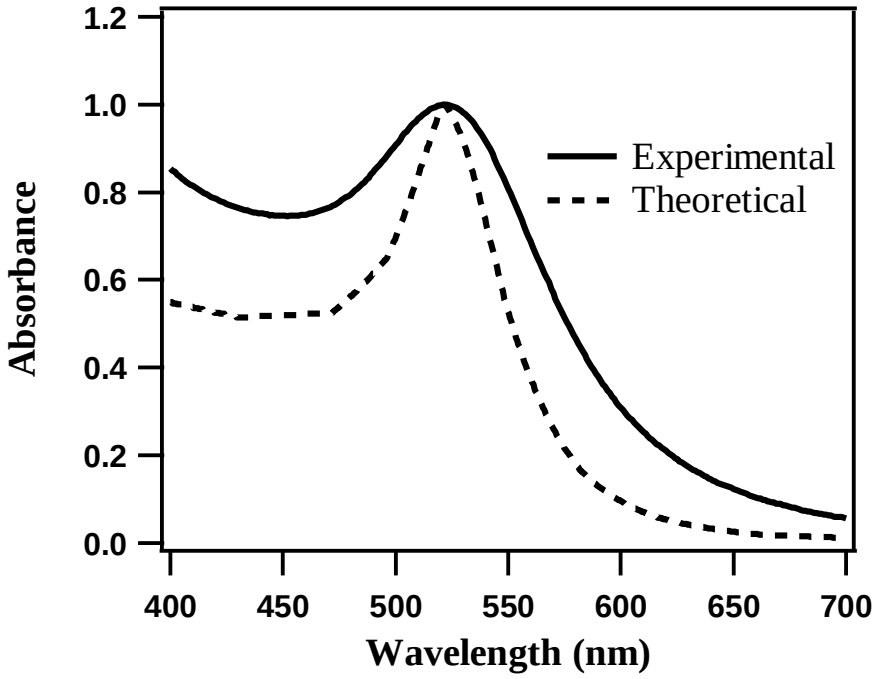

Figure S7. UV-visible absorption spectrum of Au nanoparticles. Experimental absorption spectrum (Solid line) and calculated absorption spectrum as calculated using Mieplot v4304 software for Au nanoparticles with average diameter 8.9 nm (Dashed line).

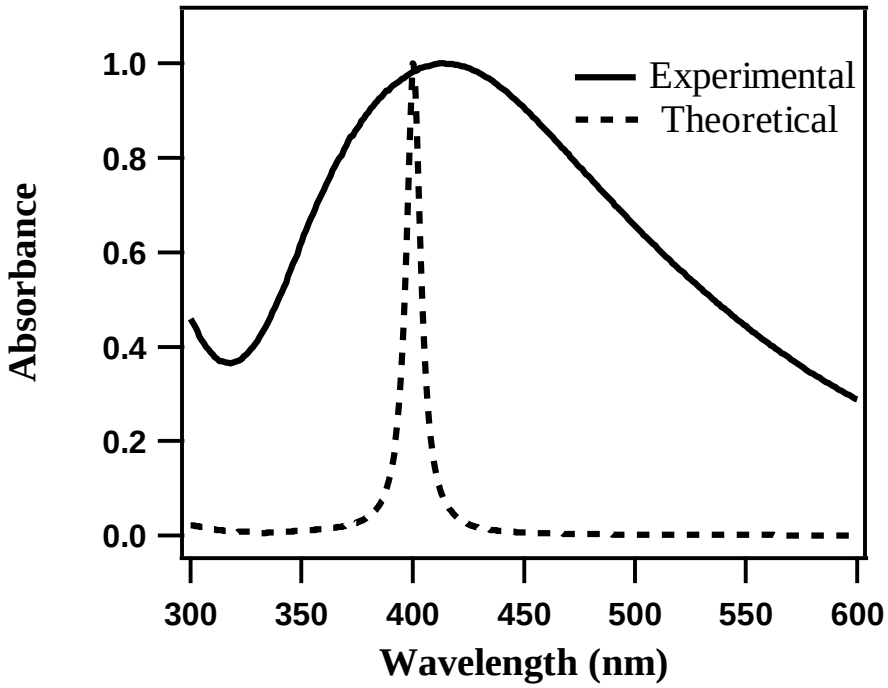

Figure S8. UV- visible absorption spectrum of Ag-Ag_2O composite nanoparticles. Experimental absorption spectrum (Solid line) and calculated absorption spectrum as calculated using Mieplot v4304 software for Ag nanoparticles with average diameter 4.1 nm (Dashed line).

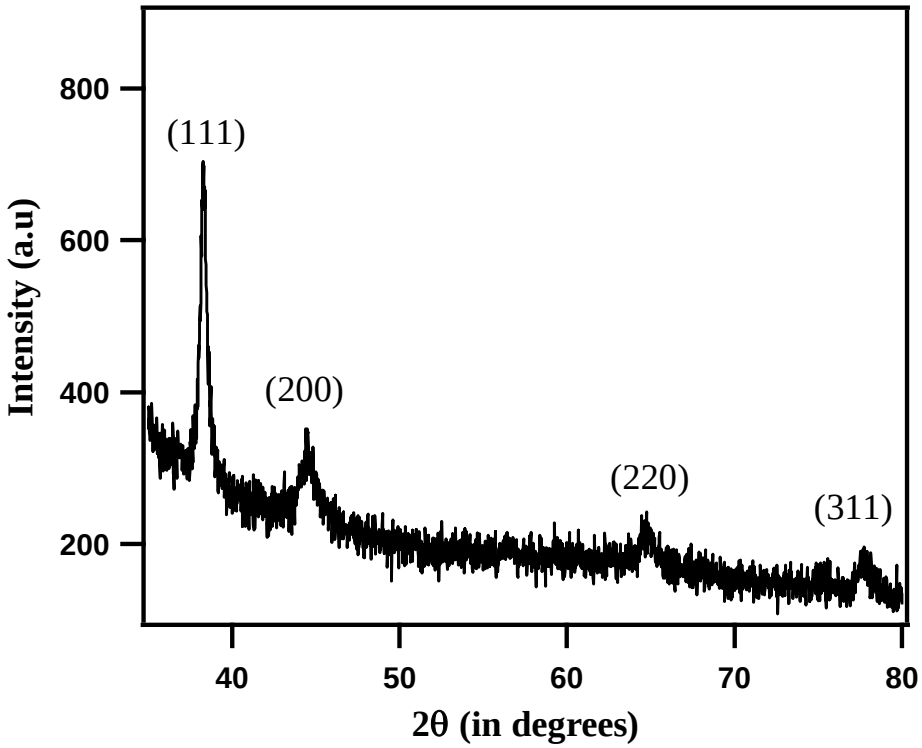

Figure S9. Powder XRD spectrum of Au nanoparticles, showing the characteristic Bragg's reflections.

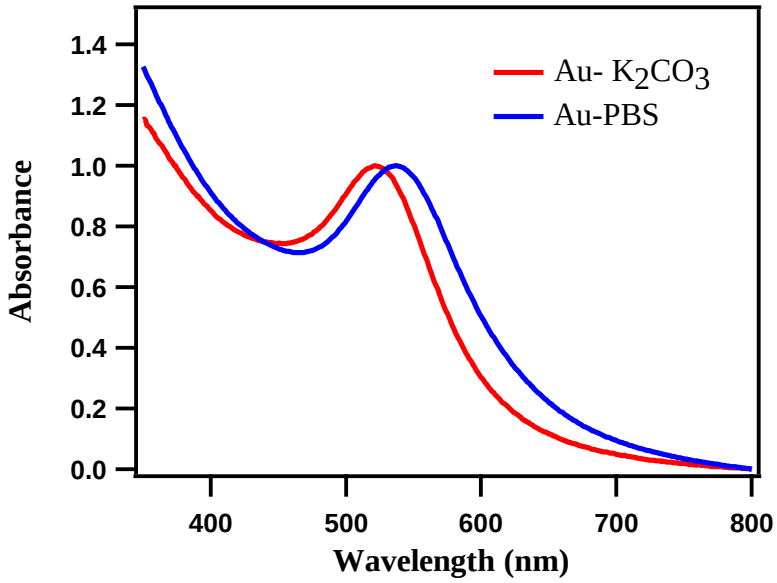

Figure S10. Normalized UV- visible spectrum of Au NPs synthesized in K_2CO_3 (λ_{max}= 522 nm) and PBS buffer (λ_{max}= 537 nm).

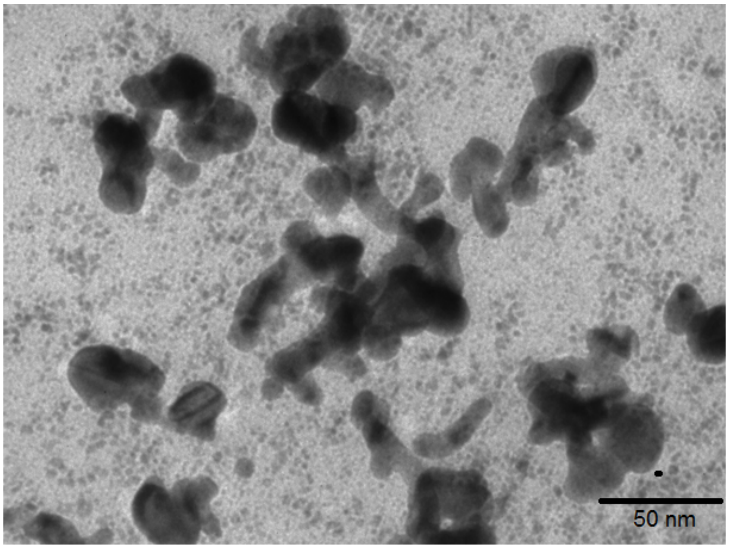

Figure S11. TEM image of Au nanoparticles synthesized in PBS, showing agglomeration.

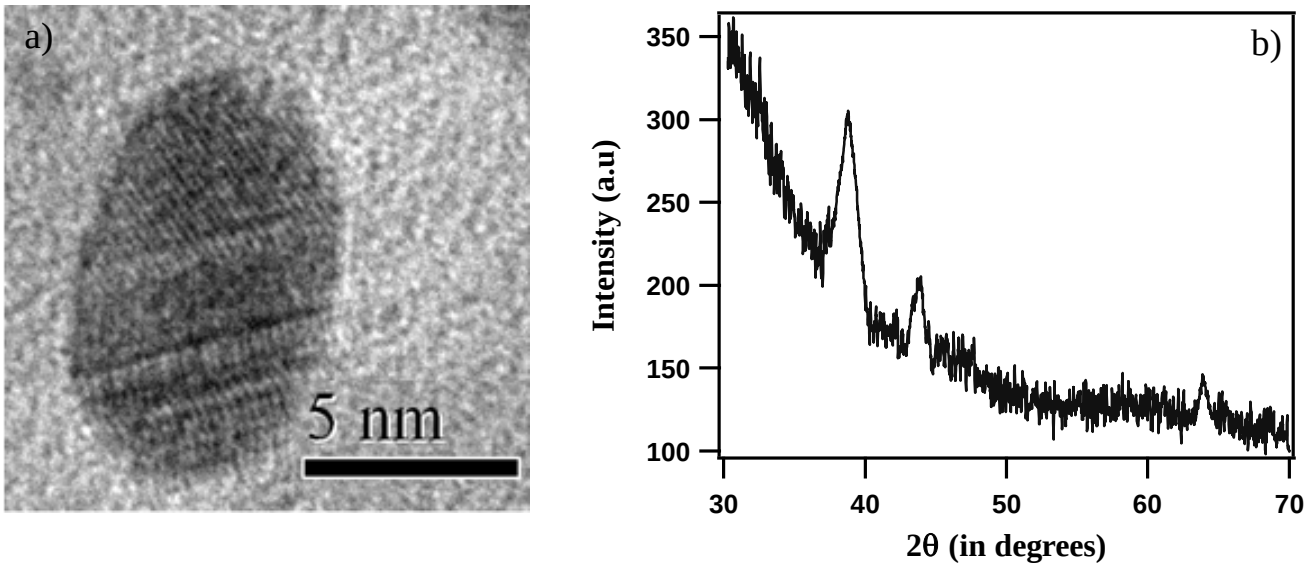

Figure S12. (a) HR-TEM image of AuAg alloy nanoparticles, showing twins and stacking faults and (b) Powder XRD spectrum of Au-Ag alloy nanoparticles.

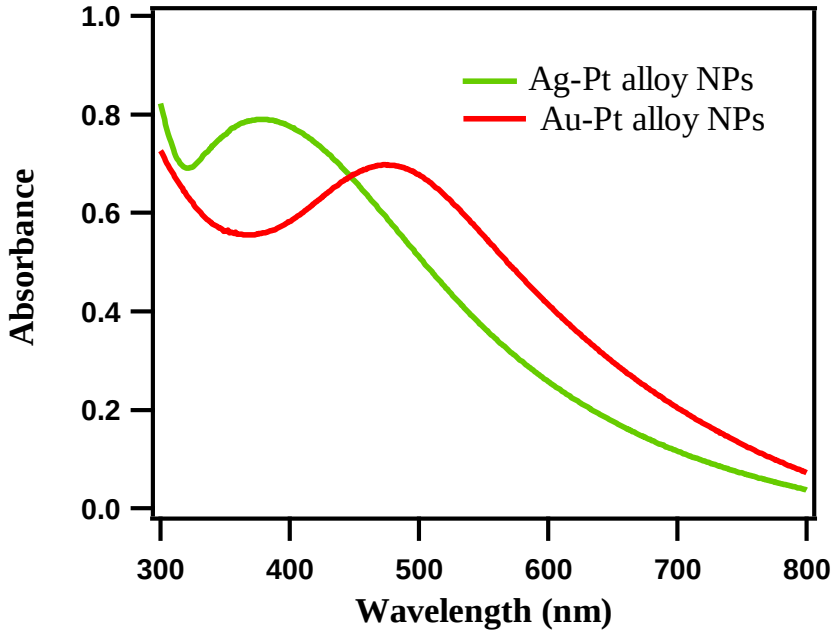

Figure S13. UV-Visible spectrum of Ag-Pt and Au-Pt alloy nanoparticles.

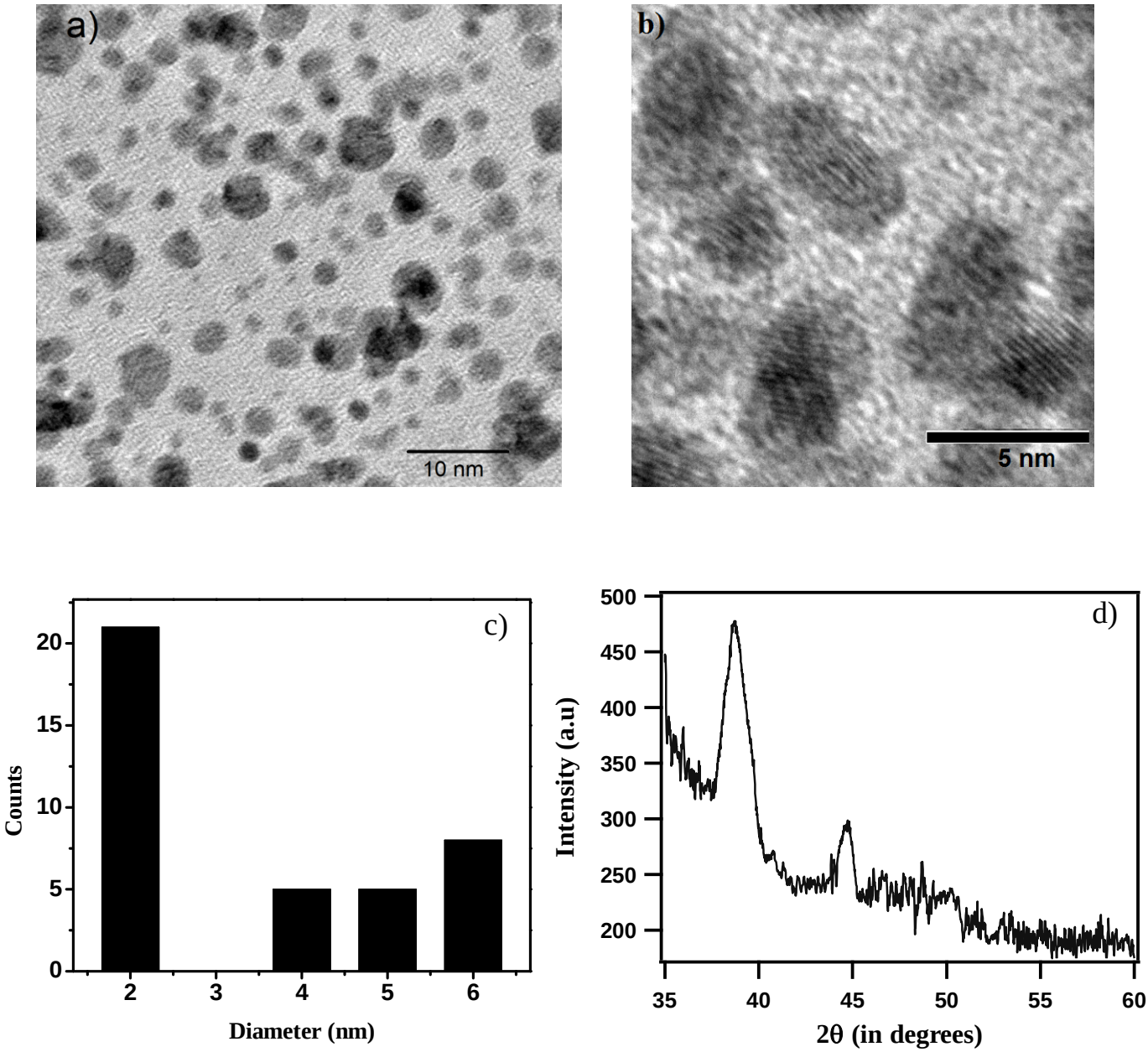

Figure S14. (a) TEM image, (b) HRTEM image, (c) particle size distribution and (d) Powder XRD spectrum of Ag-Pt alloy nanoparticles synthesized using urease.

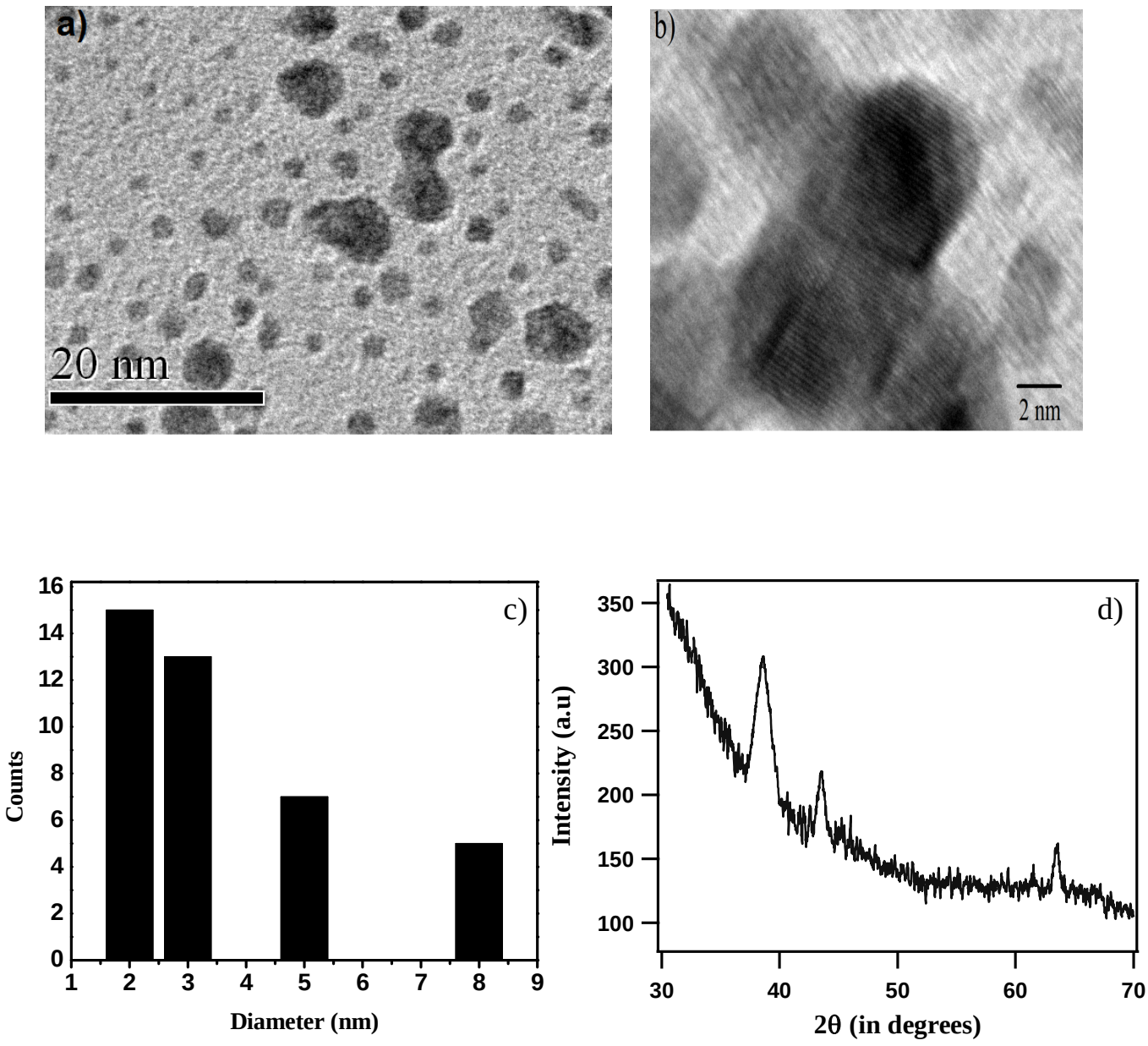

Figure S15. (a) TEM image, (b) HRTEM image (c) particle size distribution and (d) Powder XRD spectrum of Au-Pt alloy nanoparticles synthesized using urease.

Average Crystal sizes of the nanoparticles and alloys from powder-XRD measurements:

The average crystal size of all the nanoparticles was calculated from XRD using the Scherrer equation. The average crystal size for the Au, Ag and Pt nanoparticles were found to be 11.4 nm, 6.4 and 5.6 nm respectively, whereas the mean crystal size for Au-Ag, Ag-Pt and Au-Pt nanoparticles was found to be 6.4 nm, 5.4 nm and 5.6 nm respectively. The average crystal sizes of the nanoparticles from XRD were found to be a little higher compared to their mean sizes as calculated from TEM measurements. This discrepancy could be attributed to the fact that XRD size is just an approximation and is limited by the size of the particles, with no measurable signals being obtained in case of particles with sizes less than 5 nm[6]. Hence we believe that the average particle size measured from the XRD graphs are essentially from the signals obtained from the particles with larger diameter and does not represent all the nanoparticles synthesized. Thus, expectedly, the crystal size measured by XRD was found to be a little bit higher compared to the grain size as measured by TEM.

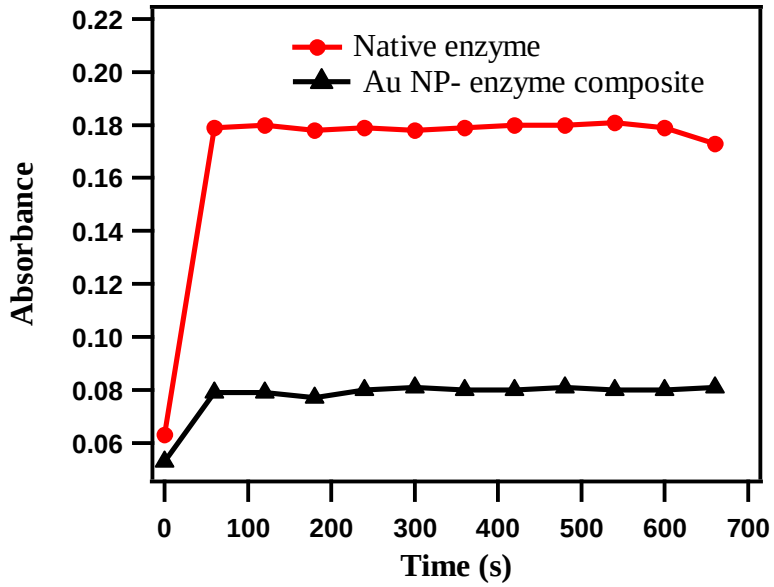

Figure S16. Comparison of the activity of native urease and urease after the synthesis of Au NPs using the dye bromocresol purple.

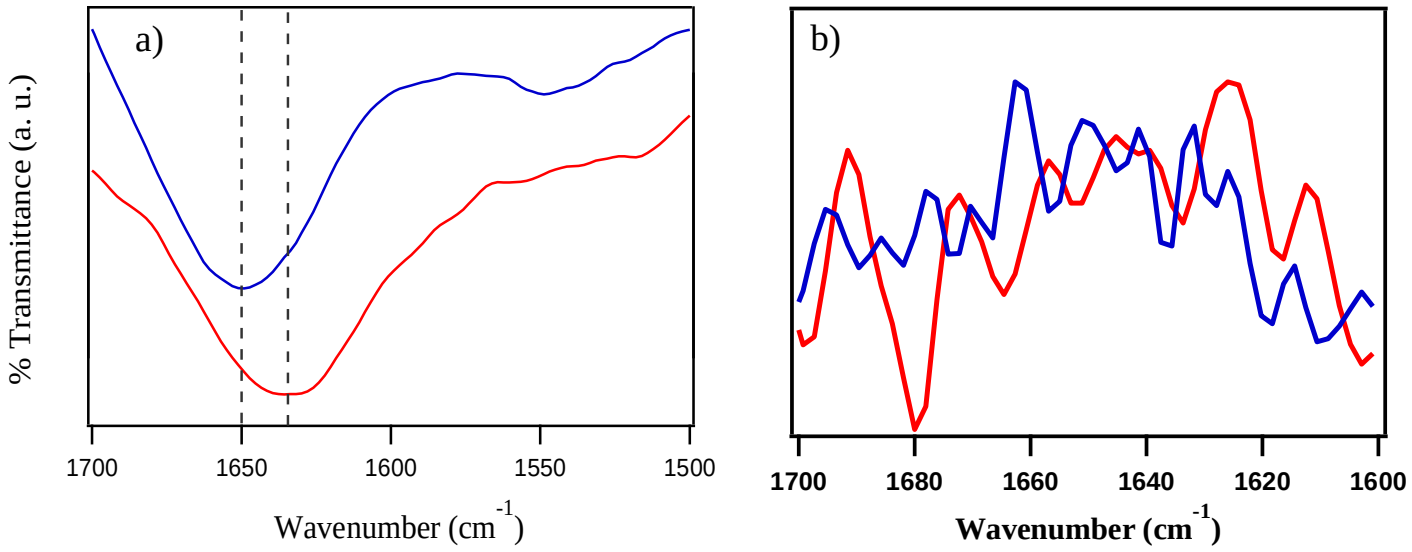

Figure S17. (a) FTIR spectrum showing the amide I and amide II region of native urease (blue line) and Au NPs- urease composite (red line) and (b) Second derivative of the amide I region of native urease (blue line) and Au NPs- urease composite (red line).

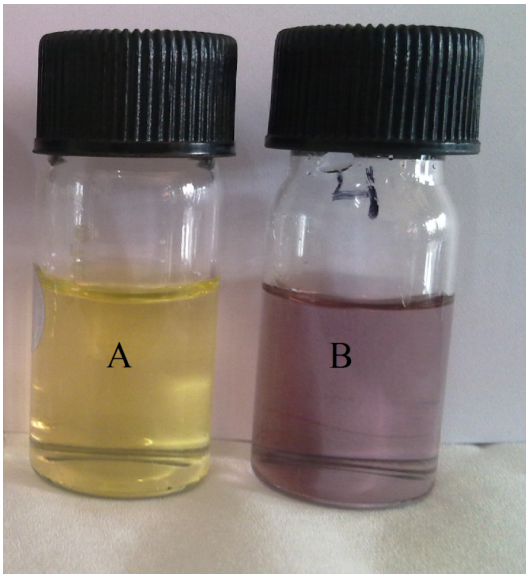

Figure S18. Photograph showing reaction of urease with $HAuCl_4$ in PBS (A) after blocking the thiol groups by DTNB and (B) unmodified urease.

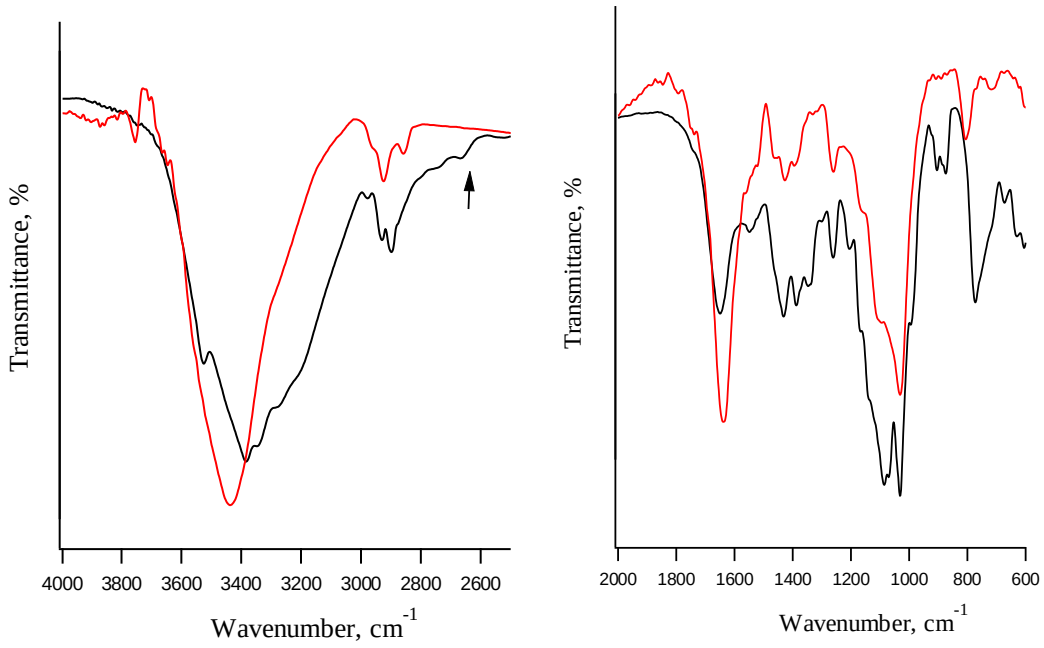

Figure S19. FTIR spectra of native urease (black line) and Au NP- urease composite (red line). (Arrow in black line shows the peak at 2660 cm^{-1} due to S-H stretching which is absent in the red line).

Modes	Native urease	Au NP- Urease composite
ν_{N-H}	3384 (s)	3433 (s)
ν_{C-H}	2930 (m)	2922 (m)
ν_{S-H}	2660 (w)	-
$\nu_{C=O}$ (amide I)	1650 (s)	1635 (s)
$\delta_{N-H} + \nu_{N-C=O}$ (amide II)	1547 (m)	1550 (w)
$\delta_{N-H} + \nu_{C-N}$ (amide III)	1260 (m)	1258 (m)

Table S1. The main vibrational modes of native urease and Au NP- urease composite.

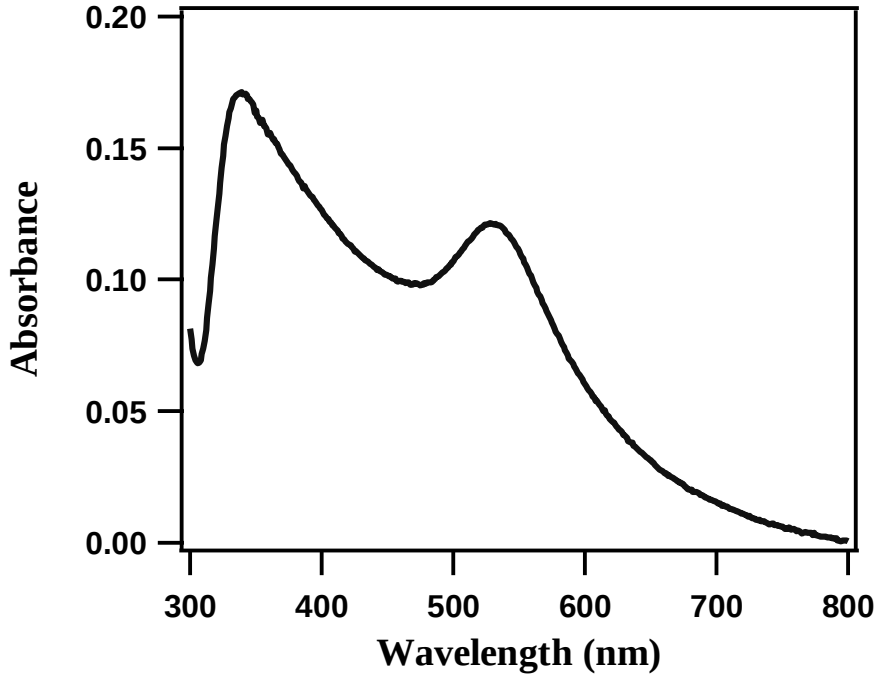

Figure S20. UV-Visible spectrum of Au@ZnO core- shell nanoparticles.

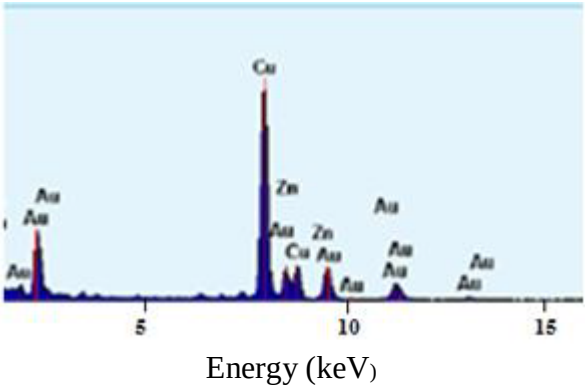

Figure S21. EDX spectrum of Au@ZnO core shell nanostructures.

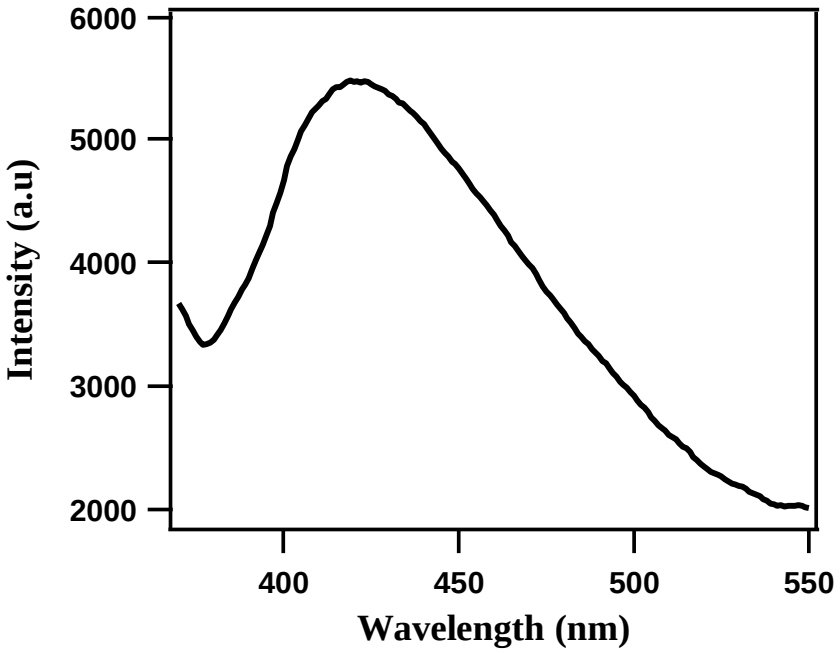

Figure S22. Fluorescence emission spectrum of Au@ZnO core shell nanoparticles (λ_{ex}=340 nm).

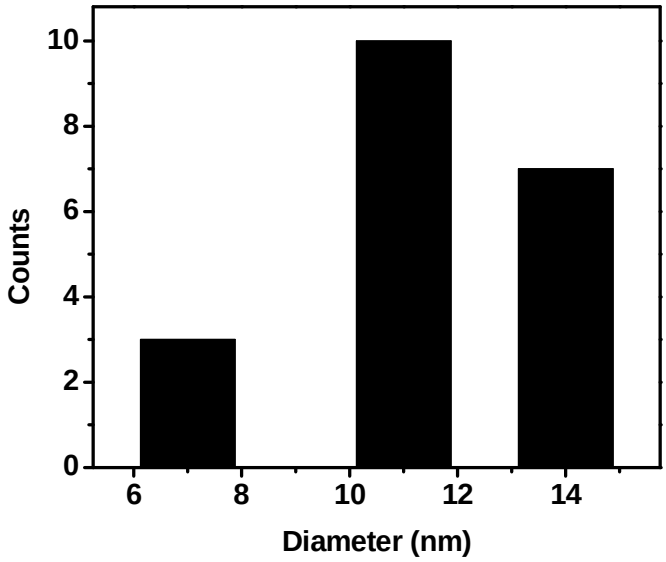

Figure S23. Particle size distribution of Au@ ZnO core shell nanoparticles.

Reduction of p-nitroaniline to 1,4-diaminobenzene with $NaBH_4$ using Au nanoparticles and Au@ZnO core shell nanoparticles as catalyst.

Au nanoparticles are well known to catalyze the reduction of p- nitroaniline to 1,4-diaminobenzene with $NaBH_4$ at room temperature[7].

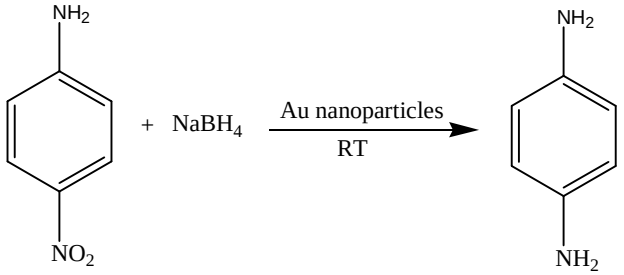

p-Nitroaniline 1,4-diaminobenzene

However, ZnO nanoparticles are not known to catalyze the same reaction. So, in order to confirm the ZnO shell on the Au nanoparticles, the reduction of *p*-nitroaniline by $NaBH_4$ with both Au nanoparticles and Au@ZnO core shell nanoparticles as catalyst was studied. It was found that in case of Au nanoparticles, the reduction was completed within 25 minutes, as evidenced by the decrease in the intensity of the peak at 380 nm and formation of a new peaks at 303 nm and 240 nm, characteristic of 1,4-diaminobenzene. However with the Au@ZnO core shell nanoparticles as catalyst, it was found that the reaction did not proceed substantially even after 10 hours, as evidenced by the absence of the peaks at 303 nm and 240 nm, but the peak at 380 nm decreased by 52% in intensity after 10 hours. For comparison, controlled experiments were performed with blank (without any nanoparticles) and ZnO-urease composite nanoparticles as catalyst. ZnO-urease nanoparticles were synthesized at pH 9.1 in water, originated from the production of ammonia due to breakdown of urea by urease. It was found that in case

of blank the intensity of the peak at 380 nm decreased by 39% after 10 hours (Figure S24a) and with ZnO-urease nanoparticles as catalysts the intensity decreased by 40% after 10 hours (Figure S24b). From the catalytic experiments (Figure 5 in the manuscript and Figure S24), the formation of ZnO shell on Au nanoparticles could be confirmed further.

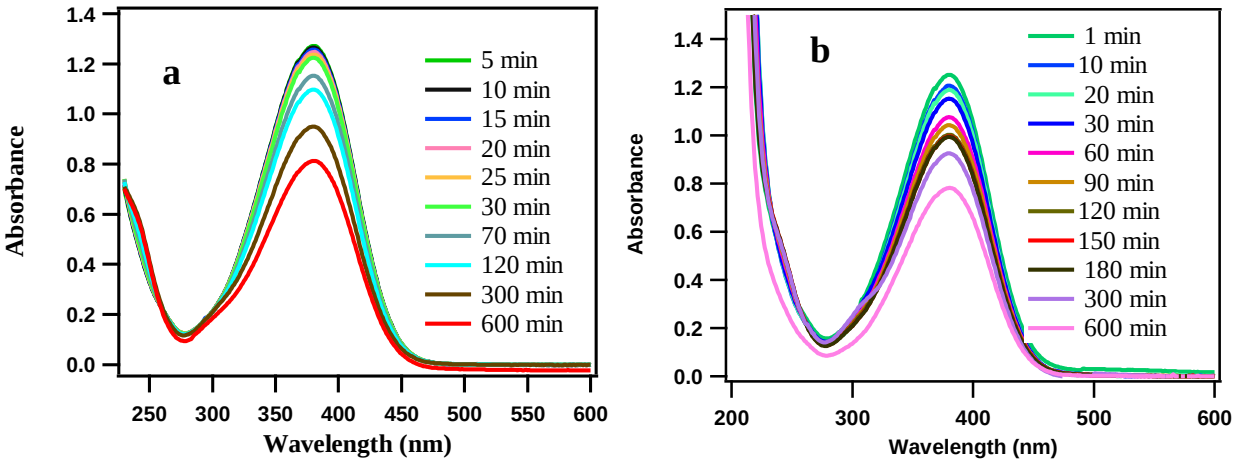

Figure S24. (a) Time-dependent UV- visible spectrum, showing the reduction of *p*-nitroaniline to 1,4-diaminobenzene with $NaBH_4$ in the absence of any nanoparticles (b) UV- visible spectrum for the reduction of *p*-nitroaniline with $NaBH_4$ in presence of ZnO-urease composite nanoparticles as catalyst.

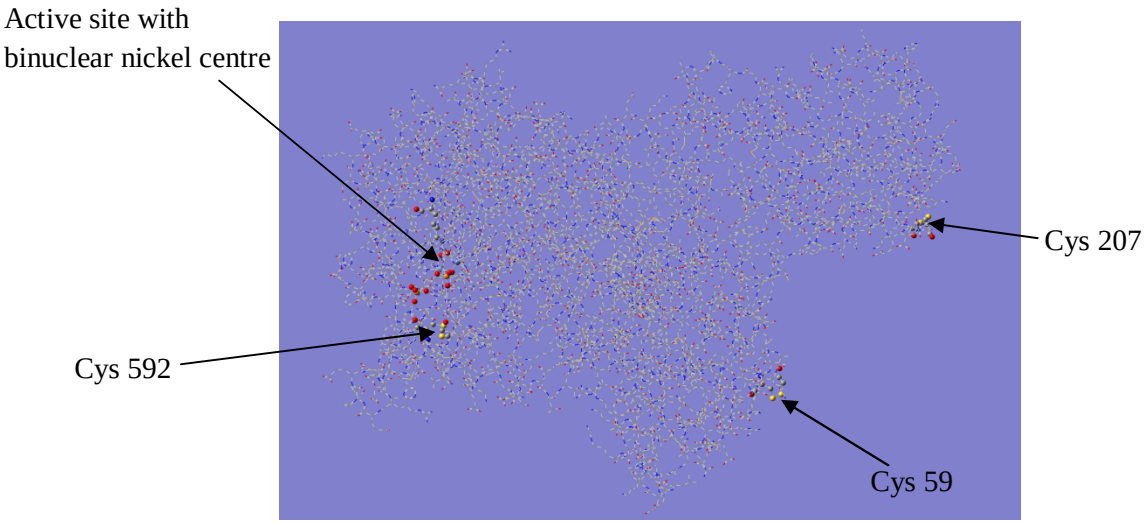

Figure S25. Overall stereo structure of the of jack bean urease. For clarity, the active site containing the binuclear Ni centre and the three reactive and exposed cysteine residues are highlighted.

Calculation of ratio of Au: Zn in Au@ZnO core shell nanoparticles

The average diameter of Au nanoparticles, d = 8.9 nm

Hence, the radius of the Au nanoparticles, r = 4.45 nm = 4.45×10^{-7} cm

∴ Volume occupied by Au nanoparticles, V = $4/3\pi r^3$ = 3.69×10^{-19} cc

Density of Au, ρ = 19.3 g/cc

∴ Mass of Au, M = V × ρ = 7.122×10^{-18}

∴ No. of moles of Au = $7.122 \times 10^{-18}/197$

= 3.62×10^{-20}moles

The average diameter of Au@ZnO core shell nanoparticles =11 nm.

Hence the radius of the Au@ZnO core shell nanoparticles = 5.5 nm

∴ Volume occupied by the ZnO shell, V = $4/3\pi r^3_{Au@ZnO} - 4/3\pi r^3_{Au}$

= $(6.95 - 3.68) \times 10^{-19}$ cc

= 3.27×10^{-19} cc

Density of Zn, ρ = 5.61 g/cc

∴ Mass of Zn, M = V × ρ = 1.834×10^{-18} g

∴ No. of moles of Zn = $1.834 \times 10^{-18}/65.38$

$$= 2.808 \times 10^{-20} \text{ moles}$$

$$\therefore \% \text{ of Au in the core shell composite} = \frac{3.62 \times 10^{-20}}{(3.62+2.808)\times 10^{-20}} \times 100$$

$$= 56.32\ \%$$

$$\text{And, \% of Zn in the core shell composite} = \frac{2.808 \times 10^{-20}}{(3.62+2.808)\times 10^{-20}} \times 100$$

$$= 43.68\ \%.$$

References:

1. Ellman, G.L. Tissue Sulphydryl Groups. *Arch. Biochem. Biophys.* **82**, 70-77 (1959).
2. Lvov, Y., Antipov, A. A., Mamedov, A., Moehwald, H. & Sukhorukov, G. B. Urease Encapsulation in Nanoorganized Microshells. *Nano Lett*. **1**, 125-128 (2001).
3. Tjeng, L. H., Meinders, M. B. J., Van Elp, J., Ghijsen, J. & Sawatzky, G. A. Electronic structure of Ag_2O. *Phys. Rev. B* **41** 3190-3199 (1990).
4. Xiao, F., Liu, H. G. & Lee, Y- III. Formation and characterization of two dimensional arrays of silver oxide nanoparticles under langmuir monolayers of n-Hexadecyl dihydrogen phosphate. *Bull. Korean. Chem. Soc.* **29**, 2368-2372 (2008).
5. Mohan, S. & Jose, G. Stability of core-shell nanoparticles formed in a dielectric medium. *Appl. Phys. Lett*. **91**, 253107 (2007).

6. Wojcieszak, R., Genet, M. J., Eloy, P., Ruiz, P. & Gaigneaux, E. M. Determination of the Size of Supported Pd Nanoparticles by X-ray Photoelectron Spectroscopy. Comparison with X-ray Diffraction, Transmission Electron Microscopy, and H2 Chemisorption Methods. *J. Phys. Chem C* **114**, 16677-16684 (2010).
7. Yao. Y *et al.* A new water-soluble pillar[5]arene: synthesis and application in the preparation of gold nanoparticles. *Chem. Commun*. **48**, 6505-6507 (2012).